ISSN 1818-331X ЯДЕРНА ФІЗИКА ТА ЕНЕРГЕТИКА 2011 Т. 12 № 4

ЯДЕРНА ФІЗИКА

УДК 539.17; 539.142; 539.172

V. M. Kolomietz

Institute for Nuclear Research, National Academy of Sciences of Ukraine, Kyiv

NON-MARKOVIAN NUCLEAR DYNAMICS

A prove of equations of motion for the nuclear shape variables which establish a direct connection of the memory effects with the dynamic distortion of the Fermi surface is suggested. The equations of motion for the nuclear Fermi liquid drop are derived from the collisional kinetic equation. In general, the corresponding equations are non-Markovian. The memory effects appear due to the Fermi surface distortions and depend on the relaxation time. The main purpose of the present work is to apply the non-Markovian dynamics to the description of the nuclear giant multipole resonances (GMR) and the large amplitude motion. We take also into consideration the random forces and concentrate on the formation of both the conservative and the friction forces to make more clear the memory effect on the nuclear dynamics. In this respect, the given approach represents an extension of the traditional liquid drop model (LDM) to the case of the nuclear Fermi liquid drop. In practical application, we pay close attention to the description of the descent of the nucleus from the fission barrier to the scission point.

Keywords: Fermi liquid, giant multipole resonances, nuclear fission, memory effects.

1. Introduction

The concept of macroscopic collective motion plays an important role in many phenomena in nuclear physics, such as large scale motion, fission, heavy ion collision, etc. Usually these phenomena are treated in terms of only a few degrees of freedom, which are chosen to describe gross properties of the nucleus [1]. Such a kind of approach is acceptable for a slow collective motion where the fast intrinsic degrees of freedom exert forces on the collective variables leading to a Markovian transport equation. An available approach to nuclear collective motion problems is still based on the standard liquid-drop model (LDM) [2, 3]. Up to now, the LDM and its extensions are widely used for the description of the main macroscopic, i.e., averaged over many quantum states, characteristics of nuclear fission [4, 5]. On the other hand, it is well known that the LDM is not able to describe some strongly collective nuclear excitations such as the giant multipole resonances (GMR) [6 - 8]. It is because the LDM ignores the important features of the nucleus as a Fermi liquid [7].

1.1. Restoring forces in a Fermi liquid

It is instructive to compare the properties of both the normal liquid drop and the Fermi liquid drop step by step. Such kind of comparison is presented in the Table. As seen from the Table, the static properties of both liquids are similar in every respect. Namely, both liquids are saturated ones, i.e., the binding energy E and the volume V are proportional to the particle number A. Moreover, the static (adiabatic) deformation energy E_{def} and the incompressibility coefficient K are the same in both liquids also.

Comparison of static and dynamic properties of the normal liquid drop and the Fermi liquid drop. The static properties are very similar in both cases whereas the dynamic ones are significantly different

Liquid drop	Fermi liquid drop
Saturation $E \sim A, \quad V \sim A$	Saturation $E \sim A, \quad V \sim A$
Static (adiabatic) deformation energy $E_{def} = E_{surf} + E_C$	Static (adiabatic) deformation energy $E_{def} = E_{surf} + E_C$
Static incompressibility $K = 9\rho^2 \partial^2 (E/A)/\partial \rho^2 \big\|_{eq}$	Static incompressibility $K = 9\rho^2 \partial^2 (E/A)/\partial \rho^2 \big\|_{eq}$
Dynamis Pressure (scalar) $P \sim \rho^{\nu}$ Shape vibrations $\omega = \sqrt{C/B}$ First sound $c_1 = \sqrt{K/9m}$ Markovian transport equations	Dynamis Pressure (tensor) $P_{\nu\mu}$ Giant resonances $\omega = \sqrt{(C + C_F)/B}$ Zero sound $c_0 \approx \sqrt{3K/9m}$ Non-Markovian motion

However the situation becomes completely different if we take a look at the dynamic behavior of both liquids. First of all, the pressure P, which is a scalar (power function) in a usual liquid, is transformed into the pressure tensor $P_{\nu\mu}$ in a Fermi liquid. In this sense, one can say that the Fermi

liquid is similar to the solid state. The origin of this phenomenon is the dynamical distortion of the Fermi surface in momentum space which accompanies the collective motion in a Fermi liquid. Due to this fact the stiffness coefficient C and the corresponding eigenfrequency ω of shape eigenvibrations are significantly different in both liquids. In a Fermi liquid, the stiffness coefficient C is subsidized by an additional strong contribution C_F because of the above mentioned Fermi surface distortion effect.

Secondly, the first sound which exists in a usual liquid is transformed to the zero sound in a Fermi liquid. The difference of both sound velocities c_1 and c_0 is related to the dynamical renormalization of the incompressibility by factor of about 3.

We will show below that the significant difference of both liquids exists also in the case of large amplitude motion, e.g. nuclear fission. In particular, the Fermi distortion effects lead to the non-Markovian equations of motion and influence strongly the descent of the nucleus from the fission barrier [9].

1.2. Non-Markovian motion

In general, the non-Markovian equations of motion imply the presence of memory effects. In the simplest case of one dimension system, such kind of non-Markovian equation reads

$$B(q)\ddot{q}+\frac{1}{2}\frac{\partial B(q)}{\partial q}\dot{q}^2=-\frac{\partial E_{pot}(q)}{\partial q}-\int_{t_0}^{t}dt'\kappa(t,t')\dot{q}(t'), \tag{1.1}$$

where $B(q)$ is the mass parameter; $E_{pot}(q)$ is the potential energy and $\kappa(t,t')$ is the memory kernel. Typically the memory kernel is taken by the exponential function as (see Refs. [10, 11])

$$\kappa(t,t')\sim\exp\left(\frac{t'-t}{\tau}\right), \tag{1.2}$$

where τ is the relaxation time.

The non-Markovian equation of motion (1.1) leads to two important consequences: (i) In a short relaxation time limit ($\tau\to 0$), Eq. (1.2) is transformed to the usual Markovian equation of motion with a friction

$$B(q)\ddot{q}+\frac{1}{2}\frac{\partial B(q)}{\partial q}\dot{q}^2+\gamma_1(q)\dot{q}=-\frac{\partial E_{pot}(q)}{\partial q}\quad(\tau\to 0), \tag{1.3}$$

where $\gamma_1(q)$ is the classical friction coefficient which is proportional to the relaxation time

$$\gamma_1(q)\sim\tau\,.$$

(ii) In an opposite limit of long relaxation time ($\tau\to\infty$), the situation is significantly different. Assuming $\tau\to\infty$, we obtain from Eq. (1.1) the following Markovian equation

$$B(q)\ddot{q}+\frac{1}{2}\frac{\partial B(q)}{\partial q}\dot{q}^2+\gamma_0(q)\dot{q}=-\frac{\partial E_{pot}(q)}{\partial q}+C_F(q),\quad(\tau\to\infty). \tag{1.4}$$

In this case, however, the friction coefficient $\gamma_0(q)$ is inverse proportional to the relaxation time similarly to the quantum mechanical principle of uncertainty

$$\gamma_0(q)\sim\frac{1}{\tau}\,.$$

Moreover, the extremely important point is that the additional force $C_F(q)$ (additional to the main driving force $-\partial E_{pot}(q)/\partial q$) appears in this case. This fact provides a lot of new features for the nuclear collective dynamics which we will discuss below.

2. Nuclear Fluid dynamics

2.1. From quantum mechanics to kinetic theory

The first question is: what is the relation of above mentioned features of Fermi liquid to the nuclear collective dynamics? In contrast to the microscopic approaches like the quantum time dependent Hartree - Fock (TDHF) approximation and its modifications [12], we will reduce the quantum equations of motion to the macroscopic ones for the collective variables. Probably, the best way to derive the corresponding macroscopic equations of motion is following, see Refs. [13 - 15]. Starting from a general quantum many-body system and performing the Wigner transform [16, 17], one can reduce the many body wave function $\Psi(\{\vec{r}_i\},t)$ to the distribution function $f(\vec{r},\vec{p};t)$ in phase space $(\vec{r},\vec{p})$:

$$\Psi(\{\vec{r}_i\},t)\ \Rightarrow\ \rho(\vec{r},\vec{r}';t)\ \Rightarrow\ f(\vec{r},\vec{p};t),$$

where $\rho(\vec{r},\vec{r}';t)$ is the one body density matrix. The many body Shrödinger equation is then transformed identically to the kinetic equation of the following form

$$\frac{\partial}{\partial t}f+\frac{1}{m}\vec{p}\cdot\vec{\nabla}_r f-\vec{\nabla}_r U\cdot\vec{\nabla}_p f=-\frac{\delta f}{\tau}+\xi, \tag{2.1}$$

where U is the selfconsistent mean field and ξ is the random force (this last one appears because of the interparticle correlations, the thermal fluctuations, etc.).

There are at least two advantages of the kinetic equation (2.1): (i) In contrast to the basic quantum Shrödinger equation, the kinetic equation (2.1) incorporates the damping effects because of the relaxation time τ. Note that within the quantum approach such kind of consideration can not be achieved directly because of Hermitian form of a quantum many-body Hamiltonian. (ii) The kinetic equation (2.1) can be easily generalized to the case of finite temperature *T*. Note also that the ensemble smearing and thereby conception of temperature can not be implanted into the quantum equations of motion in principle. Unfortunately a direct solution of the kinetic equation (1.1) is a hard problem and can be performed in some simplest cases only [18, 19].

2.2. Local equations of motion

Additional advantage of kinetic approach is the possibility to derive the macroscopic equations of motion directly starting from Eq. (2.1). One of such kind example gives the transition from Eq. (2.1) to the equations of motion for the local observable values of particle density, velocity field, pressure, etc. Taking the first three moments in $\vec{p}$-space from the kinetic Eq. (2.1), one can obtain

$$m\rho\frac{\partial}{\partial t}u_\nu + \nabla_\nu P + \nabla_\nu \frac{\delta\varepsilon_{pot}}{\delta\rho} =$$

$$= -\nabla_\mu \int_{t_0}^{t} dt' \exp\left(\frac{t'-t}{\tau}\right) P(t')\Lambda_{\nu\mu}(t') + \nabla_\nu \xi, \quad (2.2)$$

where ρ is the particle density, u_ν is the velocity field

$$u_\nu = \frac{1}{\rho}\int \frac{d\vec{p}}{(2\pi\hbar)^3}\frac{p_\nu}{m}\delta f\,,$$

P is the quantum pressure

$$P = \frac{2}{3}\varepsilon_{kin} \sim \rho^{5/3},$$

ε_{pot} is the potential energy density, ε_{kin} is the kinetic energy density and the memory tensor $\Lambda_{\nu\mu}$ is given by

$$\Lambda_{\nu\mu} = \nabla_\nu u_\mu + \nabla_\mu u_\nu - \frac{2}{3}\vec{\nabla}\cdot\vec{u}\,. \quad (2.3)$$

The integral (so called memory integral) on the right hand side of Eq. (2.2) and the memory tensor (2.3) itself occur due to the Fermi distortion effect. This effect influences the nuclear dynamics extremely strongly. We will demonstrate several examples which are related to the nuclear giant multipole resonances (GMR) and to the nuclear fission.

3. Giant multipole resonances

3.1. Shape vibrations

An instructive example of the influence of the memory and the Fermi surface distortion effects on the nuclear dynamics represents the nuclear shape vibrations (capillary waves). In Fig. 1, we show the energy of the isoscalar 2^+ collective excitations which exhaust about of 100 % sum rules.

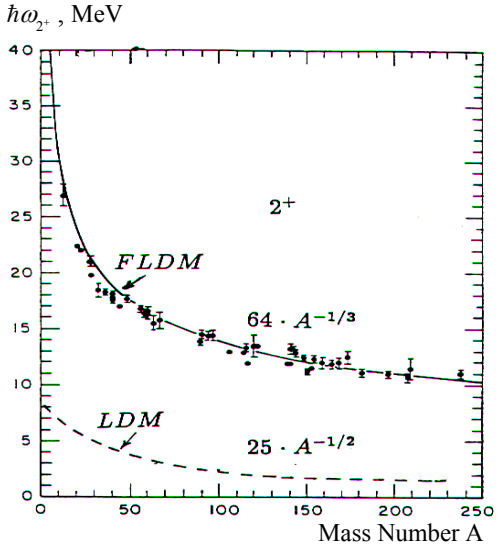

Fig. 1. Dependence of the energy $\hbar\omega_{2^+}$ of strong collectivized isoscalar 2^+ excitations on the mass number *A*. The dashed line is for the liquid drop model (LDM) and the solid line is for the Fermi liquid drop model (FLDM) where the Fermi surface distortion effects are taken into account.

The traditional liquid drop model of incompressible liquid predicts the energy behavior $\hbar\omega_{2^+} \approx 25\cdot A^{-1/2}$ MeV [3, 12] (dashed line in Fig. 1) which contradicts the experimental data for the strongly collectivized (which exhaust about 100 % of sum rules) 2^+ excitations. Taking into account the Fermi surface distortion effects and solving Eq. (2.1) we obtain the completely different *A*-dependency (solid FLDM line in Fig. 1) and the significantly higher energy $\hbar\omega_{2^+} \approx 64\cdot A^{-1/3}$ MeV which is in a very good agreement with experimental data.

The origin of this phenomenon can be easily understood if we take into consideration the following circumstance. In the Fermi liquid drop, the deformation of the surface or the distortion of the particle density in $\vec{r}$-space lead to the distortion of the Fermi surface in $\vec{p}$-space for each $\vec{r}$-point of the nuc-

leus. The distortion of the Fermi surface needs an additional potential energy and thereby leads to a shift up of the eigenenergy of the eigenvibrations. Note also that the motion in both the $\vec{r}$-space and the $\vec{p}$-space is consistent due to the relaxation time. Namely, on the distorted Fermi surface the interparticle collisions become possible and produce the two-body relaxation and the damping [20]. That leads to the damping in the basic motion in $\vec{r}$-space.

Moreover the Fermi surface distortion provides an anisotropy of the pressure tensor and increases significantly the stiffness of the nuclear surface.

3.2. Compression modes

Nuclear Fermi liquid is compressible. The incompressibility coefficient K determines the zero sound velocity c_0 and the corresponding eigenfrequencies of compression (breathing) eigenvibrations. Actually, at present one has the reliable experimental information about two kinds of compression modes, namely, the giant monopole 0^+ resonance and the isoscalar giant dipole 1^- resonance. The eigenenergies of both modes depend on the incompressibility coefficient K and this fact is usually used for the experimental determination of the nuclear incompressibility coefficient K.

However one has to be careful with such kind of determination of K. In a classical (not nuclear) liquid, we have usually a short relaxation time regime $\omega\tau \ll 1$ and the eigenenergy of compression mode is given by

$$\hbar\omega_{0^+} = \hbar\sqrt{\frac{K}{9m}}\,k, \qquad k \approx \frac{\pi}{R}, \qquad \omega\tau \ll 1, \qquad (3.1)$$

where k is the wave number. Thus, we have a direct relation between the eigenenergy and the stiffness coefficient K.

In contrast to this case, in a nuclear Fermi liquid (i.e., for long relaxation time regime $\omega\tau \gg 1$) we have the completely different relation between both the eigenfrequency ω_{0^+} and the incompressibility K. Namely,

$$\hbar\omega_{0^+} \approx \hbar\sqrt{\frac{3\cdot K}{9m}}\,k, \qquad k \approx \frac{\pi}{\sqrt{3}\cdot R}, \qquad \omega\tau \gg 1. \qquad (3.2)$$

Fortunately, there is a nice compensation of the renormalization factor ≈ 3 at the incompressibility (the value of $3K$ in Eq. (3.2) instead of K in Eq. (3.1)) due to the reducing of the wave number k and the final result for $\hbar\omega_{0^+}$ is similar to the normal liquid given by Eq. (3.1).

An important point is that such kind of compensation of the incompressibility growth exists for the main tone only but not for the overtones. In this respect, it is interesting to consider the isoscalar giant dipole resonance which is the overtone to the spurious 1^- main tone. (The spurious 1^- main tone represents the translation of the nucleus as the whole with zero's excitation energy.) In Fig. 2 we show the ratio of the energy centroids for the isoscalar E0 and E1 giant resonances [21].

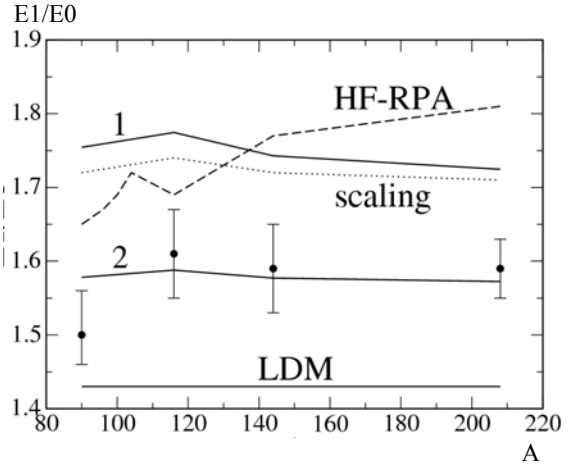

Fig. 2. Dependence of the energy ratio E1/E0 on the nuclear mass number A. The ratio of the LDM is obtained within the framework of a standard liquid drop model. The solid lines *1* and *2* are obtained from Fermi liquid drop model for $\tau \to \infty$ (solid line 1) and for realistic relaxation time $\tau = 8\cdot 10^{-23} s$ (solid line *2*). The ratio HF-RPA (dashed line) is from fully self-consistent RPA calculations.

In agreement with the above mentioned compensation effect, the dipole compression mode should be additionally shifted up with respect to the monopole one. This fact is reflected in Fig. 2 where the curve *1* (pure Fermi liquid calculation without damping, i.e., for $\tau \to \infty$) is strongly shifted up with respect to the liquid drop model calculations (solid line LDM). Note that the quantum RPA calculations, where the damping effects are neglected, give the shift up for the ratio E1/E0 also. A good agreement with experimental data is obtained within the Fermi liquid approach if the relaxation (damping effect) is taken into account (see solid line *2* in Fig. 2).

3.3. Isovector mode

Fermi liquid approach can be also applied to the isovector excitations where the proton and neutron liquids are shifted in opposite directions. The restoring force is determined here by the symmetry energy

$$b_{sym} = b_{sym,vol} + b_{sym,surf}\,A^{-1/3} + b_{sym,F}(A), \qquad (3.3)$$

where $b_{sym,vol}$ and $b_{sym,surf}$ are the volume and surface contributions to the symmetry energy, and $b_{sym,F}(A)$

is the contribution from the Fermi surface distortion. As above mentioned, the Fermi liquid has some features of the solid state because of the Fermi surface distortion effects. Due to this fact, the isovector mode in a nuclear Fermi liquid represents a combination of both the Steinwedel - Jensen mode and Goldhaber - Teller one. This peculiarity of the Fermi liquid approach provides a good description of A-dependency for the light and heavy nuclei simultaneously [22]. It is shown in Fig. 3.

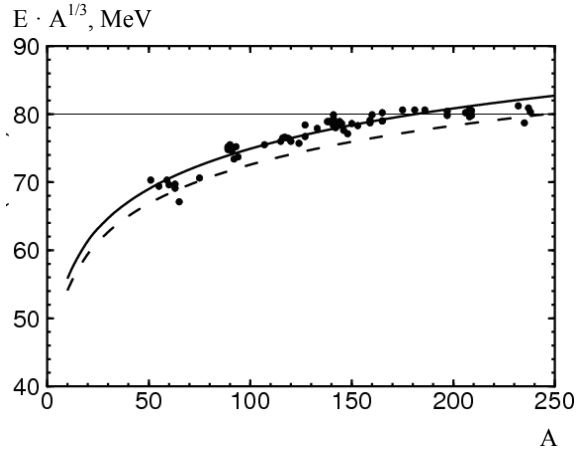

Fig. 3. Dependence of the energy of isovector dipole giant resonance on the mass number A: the dashed line is the calculation which includes the Fermi surface deformation up to a quadrupole one (scaling approximation); the solid line was obtained within Fermi liquid model without restrictions on the multipolarity of the Fermi surface distortions; the solid straight line is the traditional LDM result $E \approx 80 \cdot A^{-1/3}$MeV [3].

The Fermi liquid approach allows one to reproduce the A-dependency of the enhancement factor for so-called model-independent sum rule m_1. Note that in contrast to the isoscalar dipole mode where the sum m_1 is really model-independent, the value of m_1 is actually model-dependent for the isovector dipole excitations. The energy weighted sum m_1 is related to the photoabsorption cross-section $\sigma_{abs}(\omega)$ of γ-quanta as following [22]

$$m_1 = \int_0^\infty d(\hbar\omega)\,\sigma_{abs}(\omega) = \frac{2\pi^2\hbar e^2}{mc}\frac{NZ}{A}\left[1+\kappa(A)\right],$$

where $1+\kappa(A)$ is the enhancement factor with respect to the classical Thomas - Reiche - Khun (TRK) sum rule. In the isoscalar case, the enhancement factor is absent and $\kappa(A)=0$, i.e., m_1 sum rule is really model independent. In contrast to that, in the isovector case, one has $\kappa(A)\neq 0$. The origin of non-zero value of $\kappa(A)\neq 0$ is the velocity dependency of the inter-nucleon interaction and the fact that the nucleon effective mass in the isovector channel is different than the one for the isoscalar excitations.

The enhancement factor $1+\kappa(A)$ for the isovector giant dipole resonances is shown in Fig. 4.

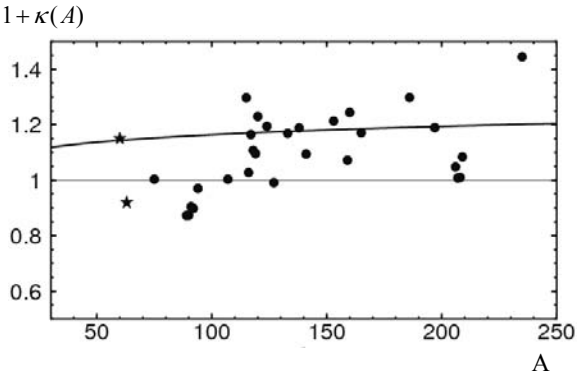

Fig. 4. Dependence of the enhancement factor $1+\kappa(A)$ for the isovector dipole giant resonance on the mass number A obtained within Fermi liquid approach (solid line). The dashed line is the microscopic RPA calculations with Skyrme forces. The solid points are the experimental data of the Livermore group.

An extraction of A-dependency of the enhancement factor $1+\kappa(A)$ from the experimental data is not a simple problem. The experimental data has no a good accuracy yet. Note that the standard RPA calculations overestimate the enhancement factor and the Fermi liquid results of Fig. 4 are more appropriate.

4. Large amplitude motion

As it was mentioned in Sect. 3, the collective motion of the nuclear Fermi liquid is accompanied by the dynamical distortion of the Fermi surface and the collective potential energy E_{pot} is subsidized by an additional contribution, $E_{pot,F}$ because of the dynamic Fermi surface deformation. The energy $E_{pot,F}$ is a smooth quantity (in sense of the quantum shell oscillations) and it can not be recovered taking into consideration the quantum shell corrections to the adiabatic (static) potential energy deformation. This fact creates the following problem.

The LDM deformation energy $\tilde{E}_{def}$ has a minimum for a sphere, i.e., for $q=0$. The total deformation energy

$$E_{def}(q) = \tilde{E}_{def}(q) + \delta U(q) \qquad (4.1)$$

includes both the smooth part $\tilde{E}_{def}$ and the irregular shell correction $\delta U(q)$ [26]. The shell correction $\delta U(q)$ provides two effects: a shift of the ground

state to values of $q \neq 0$ and an appearance of the second minimum in $E_{def}(q)$ (super-deformation). Note, however, that the practical calculations of the deformation energy $E_{def}(q)$ assumes always the presence of the external cranking field which disappears in the stationary points of minima and maxima of energy $E_{def}(q)$ only. Both the shell correction method and the constrained Hartree – Fock approximation are not free from this inconvenience. The behavior of deformation energy $E_{def}(q)$ between the stationary points where $\partial E_{def}(q)/\partial q = 0$ is still a puzzle which has no solution yet. Another problem occurs on the distant right slope of curve $E_{def}(q)$, i.e., in the case of the descent of the nucleus from the barrier to the scission point.

Considering the nuclear shape deformation near the LDM ground state at $q = 0$, we saw earlier (see Fig. 1) the strong increase of the surface stiffness coefficient due to the Fermi surface distortion effect and the corresponding shift of the energy of the surface eigenvibrations from the region of $1 \div 2\,\mathrm{MeV}$ to $10 \div 15\,\mathrm{MeV}$. On the right slope of the fission barrier one can also expect that the same dynamical Fermi surface distortion effects should influence the descent of the nucleus from the fission barrier. The following problem can occur in this case. If the deformation energy E_{def} is given by Eq. (4.1), then the question is how the smooth energy $\tilde{E}_{def}$ looks like. Does this smooth energy equal to the adiabatic liquid drop energy or to the energy of the Fermi liquid drop which includes the additional contribution from the Fermi surface distortion effect?

To answer this question we have to derive the equations of motion for the shape variables which can be applied to the large amplitude motion. Assuming the incompressible nuclear Fermi liquid and reducing the above established non-Markovian local equations of motion (2.2) for the velocity field, one can obtain the following quite general macroscopic equations of motion [9 - 11]

$$\sum_{j=1}^{N}\left[B_{ij}(q)\ddot{q}_j + \frac{1}{2}\sum_{k=1}^{N}\frac{\partial B_{ij}(q)}{\partial q_k}\dot{q}_j\dot{q}_k \right] +$$

$$+\sum_{j=1}^{N}\int_{t_0}^{t} dt' \exp\left(\frac{t'-t}{\tau}\right)\kappa_{ij}(t,t')\,\dot{q}_j(t') = -\frac{\partial \tilde{E}_{pot}(q)}{\partial q_i} + \xi_i(t), \tag{4.2}$$

where $\kappa_{ij}(t,t')$ is the memory tensor and $\xi_i(t)$ is the random force which satisfies the following property for the ensemble smearing

$$\left\langle \xi_i(t) \right\rangle = 0, \quad \left\langle \xi_i(t)\xi_j(t') \right\rangle \sim T \exp\left(-\frac{|t-t'|}{\tau} \right)\delta_{ij}, \tag{4.3}$$

where $\langle ... \rangle$ means the ensemble smearing.

The non-Markovian Langeven Eqs. (4.2) can be solved directly. The mass tensor $B_{ij}(q)$ is usually evaluated taking into account the vortex motion also. The driving force $-\partial \tilde{E}_{pot}(q)/\partial q_i$ can be taken from the liquid drop model. A new element in Eq. (4.2) is the memory integral which provides the contribution to both the conservative (elastic), $F_{i,cons}(q,t)$, and the dissipative (friction), $F_{i,dis}(q,t)$, forces

$$\sum_{j=1}^{N}\int_{t_0}^{t} dt' \exp\left(\frac{t'-t}{\tau}\right)\kappa_{ij}(t,t')\,\dot{q}_j(t') =$$

$$= F_{i,cons}(q,t) + F_{i,dis}(q,t). \tag{4.4}$$

It can be shown that the conservative time-reversible elastic force $F_{i,cons}(q,t)$ acts against the driving force $-\partial \tilde{E}_{pot}(q)/\partial q_i$ always. That creates the effect of a hindrance to the fission for the descent from the fission barrier to the scission point. This effect depends on both the collective velocity and the relaxation time. In the case of slow motion the hindrance is absent similarly to the first sound regime for small amplitude vibrations. The hindrance effect grows if the collective velocity is growing. Due to this peculiarity, the velocity of descent goes down, i.e., the hindrance effect becomes weaker and the nucleus starts to accelerate again, etc. Such kind of change of the hindrance effect along the descent trajectory leads to the characteristic shape oscillations which accompany the descent of the nucleus from the fission barrier [9].

4.1. Descent from the fission barrier

We will apply the non-Markovian approach to the symmetric nuclear fission in two dimension case. The shape of the fissionable nucleus is derived by the rotation of the profile function $Y(z;\{q_i(t)\})$ in the following form

$$Y(z,\{q_i(t)\}) \equiv Y(z;\zeta_0,\zeta_2) = \frac{(z^2-\zeta_0^2)(z^2+\zeta_2^2)}{Q}, \tag{4.5}$$

where the multiplier Q guarantees the volume conservation,

$$Q = -\frac{\zeta_0^3\left(\zeta_0^2/5 + \zeta_2^2\right)}{R_0^3}.$$

Here, all quantities of the length dimension are expressed in the R_0 units. The parameter ζ_0 determines the general elongation of the figure and ζ_2 is related to the radius of the neck. For $\zeta_2 = \infty$, the shapes coincide with the spheroidal ones. At finite ζ_2 ($\zeta_2 > 0$ for bound figures) the neck appears and the value $\zeta_2 = 0$ corresponds to the scission point after which the figure is divided in the two parts for $\zeta_2 < 0$.

To make the discussion more clear we compare both the non-Markovian (Fermi liquid drop model) and the Markovian (traditional liquid drop model) results. For a moment, we restrict ourselves by the one dimension case. The Markovian limit is obtained from Eq. (4.2) for $\tau \to 0$ and reads

$$B(q)\ddot{q} + \frac{1}{2}\frac{\partial B(q)}{\partial q}\dot{q}^2 = -\frac{\partial \tilde{E}_{pot}(q)}{\partial q} - \gamma(q)\dot{q}\,, \qquad (4.6)$$

where $\gamma(q)$ is the friction coefficient

$$\gamma = \omega_F B \frac{\omega_F \tau}{1+(\omega_F \tau)^2},\ \omega_F = \sqrt{\kappa_0 / B},\ \kappa_0 = \frac{4}{5m}\pi\rho_0 p_F^2 R_0^3. \qquad (4.7)$$

The numerical calculations of Ref. [9] for the one dimension motion (descent from barrier) near the saddle point shows two consequences of the memory effect (Fermi surface distortion effect): (i) The descent is strongly hindered due to the Fermi surface distortion effect, (ii) The memory effects lead to the characteristic oscillations of nuclear shape. The time dependency of shape parameter is then given by

$$\Delta q(t) = C_\zeta e^{\zeta t} + A_\omega e^{-\Gamma t/2\hbar}\sin(Et/\hbar) + \\ + B_\omega e^{-\Gamma t/2\hbar}\cos(Et/\hbar)\,, \qquad (4.8)$$

where ζ is the instability growth rate, $E/\hbar$ is the characteristic eigenfrequency and Γ is the damping width. All these values depend on the relaxation time τ. For realistic value of the relaxation time $\tau \approx 8\cdot 10^{-23}$s, we can expect the accompanied characteristic oscillations with the eigenenergy $E \approx 6 \div 7$MeV. That is quite below a typical energy of giant resonances and exceeds the energy of thermal gamma-quanta. The intriguing problem is to study experimentally the corresponding gamma-quanta emission which accompanies the descent of the nucleus from the fission barrier (pre-scission γ-quanta).

The profile function of Eq. (4.5) provides the descent of the nucleus in two-dimension space of shape variables: $q = \{q_1, q_2\} = \{\zeta_0, \zeta_2\}$. The fission point is derived by the condition of the disappearance of the restoring force with respect to neck radius. The corresponding condition reads

$$\frac{\partial^2 E_{pot}(q)}{\partial \zeta_2^2} = 0\,. \qquad (4.9)$$

The separation of fissionable nucleus in two fragments happens in the crossing point of both the trajectory (obtained from Eq. (4.2)) and the scission line (obtained from Eq. (4.9)). In the long relaxation time regime, the memory effects hinder strongly the descent of the nucleus from the fission barrier with respect to the usual liquid drop model with friction. For the realistic relaxation time $\tau \approx 8\cdot 10^{-23}$s [23 - 25] one has a factor about of 2 for the hindrance effect [9]. This hindrance is because of the Fermi distortion effect. The Fermi distortions produce, as it was above mentioned, the conservative (elastic) force which works against the usual driving force occurred on the adiabatic fission barrier.

This fact is extremely important for understanding of the energy balance at the scission point and the yield of the kinetic energy of the fission fragments. The most probable total kinetic energy (TKE) of fission fragments is given by

$$E_{kin} = E_{Coul} + E_{kin,ps}\,, \qquad (4.10)$$

where E_{Coul} is the repulsive Coulomb energy at the scission point and $E_{kin,ps}$ is the pre-scission kinetic energy. The energy E_{kin} depends on the redistribution of the potential energy, ΔE_{pot}, which is released from the fission barrier among different components. Namely, the following energy balance exists at fission point

$$\Delta E_{pot} = E_{kin,ps} + E_{dis} + E_{F,ps}\,, \qquad (4.11)$$

where E_{diss} is the dissipation energy and $E_{F,ps}$ is the energy which is collected (at scission point) as the potential energy due to the Fermi surface deformation. In contrast to dissipation energy E_{diss}, the potential energy $E_{F,ps}$ is time reversible, i.e., it is not transformed to the heat. The balance of energies is illustrated in Fig. 5.

It is seen from Fig. 5 that the presence of memory effects (solid line) leads to a decrease of the pre-scission kinetic energy. This is because a significant part of the potential energy ΔE_{pot} at the scission point is collected as the energy of the Fermi surface deformation. Due to this fact, the nucleus loses a

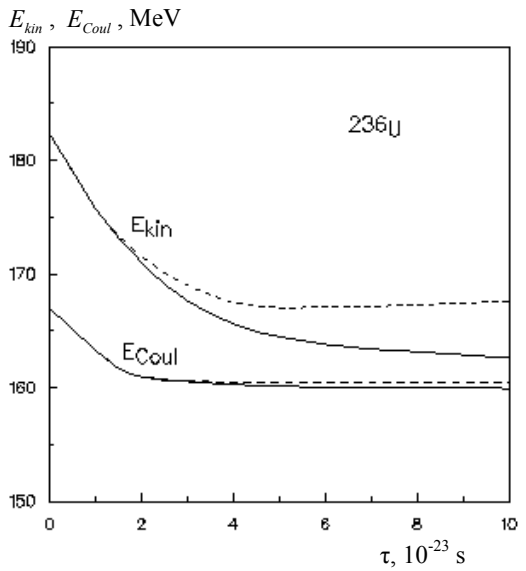

Fig. 5. Fission-fragment kinetic energy, E_{kin}, and the Coulomb repulsive energy at the scission point, E_{Coul}, versus the relaxation time τ for the nucleus ^{236}U. The solid lines represent the result of the calculation in presence of the memory effects and the dashed lines are for the case of Markovian (no memory) motion with the friction forces.

part of the pre-scission kinetic energy converting it into the potential energy of the Fermi surface distortion instead of the time-irreversible heating of the nucleus. A good agreement with the experimental value for the TKE is obtained for a moderate value of the relaxation time $\tau \approx 8 \cdot 10^{-23}$s. Note that to achieve such kind of result within the traditional liquid drop model the over-damped motion for the descent from the fission barrier is usually assumed.

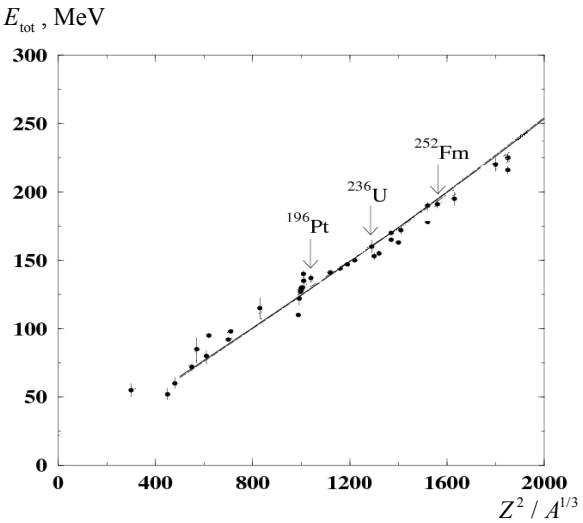

Fig. 6. The most probable total kinetic energy (TKE) E_{tot} of fission versus the fission parameter $Z^2 / A^{1/3}$ within the Fermi liquid drop model for the relaxation time $\tau = 8 \cdot 10^{-23}$s.

The agreement of the non-Markovian calculations of the TKE in actinide nuclei with experimental data is shown in Fig. 6. All numerical calculations were here performed for the relaxation time $\tau \approx 8 \cdot 10^{-23}$s which corresponds to the moderate friction (damping) in fissionable nucleus.

That is important from point of view of consistency of theory. In particular, using the same value of the relaxation time $\tau = 8 \cdot 10^{-23} s$ we have to be able to reproduce the widths of the giant multipole resonances.

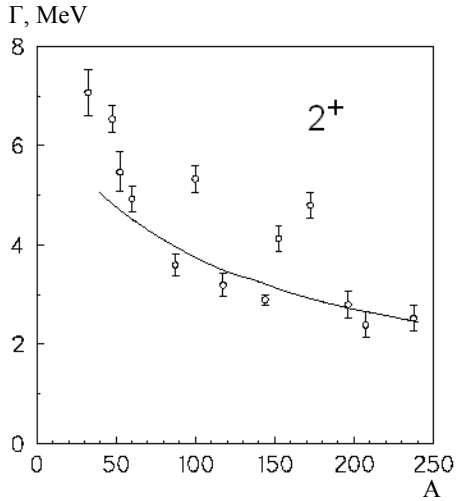

Fig. 7. The collisional width of the giant quadrupole resonance within the Fermi-liquid drop model for the relaxation time $\tau = 8 \cdot 10^{-23}$s (solid line).

This possibility is demonstrated in Fig. 7 for the isoscalar giant quadrupole resonances. We point out that the use of the friction coefficient obtained from a fit of the TKE to the experimental data within the traditional (not Fermi-liquid) liquid drop model leads to a significant overestimate of the widths of the giant multipole resonances.

5. Conclusions

The collective motion of the nuclear Fermi liquid is accompanied by the dynamical distortion of the Fermi surface. In general, the corresponding macroscopic equations of motion are non-Markovian and contain the memory integral which is caused by the Fermi surface distortions and depends on the relaxation time τ. The memory effects on the nuclear collective motion disappear in two limits: at zero relaxation time, $\tau \to 0$, and at $\tau \to \infty$. The memory integral contains the contribution from both the time reversible elastic force and the dissipative friction force.

The eigenmotion near the ground state of the nuclear Fermi-liquid drop is influenced by the memory effects through both the additional contribution

to the stiffness, C_F, and to the friction coefficient γ. In the rare collision limit of $\tau \to \infty$, the additional contribution (elastic force) appears due to the memory integral. The contribution from the elastic force is significantly stronger than the one caused by the adiabatic driving force. The presence of the elastic force provides a correct A-dependence of the energy of the giant multipole resonances.

The development of instability near the fission barrier is strongly influenced by the memory effects if the relaxation time τ is large enough. In such a case, a drift of the nucleus from the barrier to the scission point is accompanied by characteristic shape oscillations which depend on the memory kernel and on the relaxation time τ. The shape oscillations appear due to the elastic force induced by the memory integral. The elastic force acts against the adiabatic force $-\partial E_{pot}(q)/\partial q$ and hinders the motion to the scission point. In contrast to the case of the Markovian motion, the delay in the fission is caused here by the conservative elastic force but not only by the friction force. Due to this fact, the nucleus loses a part of the pre-scission kinetic energy converting it into the potential energy of the Fermi surface distortion instead of the time-irreversible heating of the nucleus. In contrast to the Markovian motion, the memory effects provide a monotonous dependence of the saddle-to-scission time on the relaxation time τ. This is caused by the elastic forces produced by the memory integral, which lead to the additional hindrance effect for the descent from the barrier at large τ.

The memory effects lead to the decrease of the fission-fragment kinetic energy, E_{kin}, with respect to the one obtained from the Markovian motion with friction. This is because a significant part of the potential energy at the scission point is collected as the energy of the Fermi surface deformation. Note that the decrease of the fission-fragment kinetic energy due to the memory effects is enhanced in the rare collision regime (at larger relaxation time) while the effect due to friction decreases.

We pointed out also that the Fermi liquid drop model provides a consistent description of the dissipation processes in completely different fields of nuclear dynamics. Namely, both the kinetic energy fission fragments and the widths of giant multipole resonances can be described assuming the same value of the collisional relaxation time.

REFERENCES

1. *Hasse R.W., Myers W.D.* Geometrical Relationships of Macroscopic Nuclear Physics. - Berlin: Springer-Verlag, 1988. - 296 p.
2. *Myers W.D., Swiatecki W.J.* The nuclear drop model for arbitrary shapes // Ann. of Phys. - 1967. - Vol. 84. - P. 186 - 210.
3. *Бор О., Моттельсон Б.* Структура атомного ядра. - Т. 2. - М.: Мир, 1977. - 664 с.
4. *Nix J.R., Sierk A. J., Hofmann H. et al.* Stationary Fokker - Planck equation applied to fission dynamics // Nucl. Phys. A. - 1984. - Vol. 424, No. 2. - P. 239 - 261.
5. *Ivanyuk F.A., Kolomietz V.M., Magner A.G.* Liquid drop surface dynamics for large nuclear deformations // Phys. Rev. C. - 1995. - Vol. 52, No. 2. - P. 678 - 684.
6. *Nix J.R., Sierk A.J.* Microscopic description of isoscalar giant multipole resonances // Phys. Rev. C. - 1980. - Vol. 21, No. 1. - P. 396 - 404.
7. *Kolomietz V.M., Shlomo S.* Nuclear Fermi liquid drop model // Phys. Rep. - 2004. - Vol. **690**, No. 3. - P. 133 - 233.
8. *Holzwarth G., Eckart G.* Fluid-dynamical approximation for finite Fermi systems // Nucl. Phys. A. - 1979. - Vol. 325, No. 1. - P. 1 - 30.
9. *Kolomietz V.M., Radionov S.V., Shlomo S.* Memory effects on descent from nuclear fission barrier // Phys. Rev. C. - 2001. - Vol. 64, No. 5. - P. 054302.
10. *Kolomietz V.M., Åberg S., Radionov S.V.* Collective motion in quantal diffusive environment // Phys. Rev. C. - 2008. - Vol. 77, No. 1. - P. 014305(10).
11. *Kolomietz V.M., Radionov S.V., Shlomo S.* Non-Markovian Langevin dynamics of nuclear Fermi liquid drop // Physica Scripta. - 2006. - Vol. 73, No. 3. - P. 428 - 439.
12. *Ring P., Schuck P.* The Nuclear Many-Body Problem. - Berlin: Springer-Verlag, 1980. - 711 p.
13. *Kolomietz V.M., Tang H.H.K.* Microscopic and macroscopic aspects of nuclear dynamics in mean-field approximation // Physica Scripta. - 1981. - Vol. 24, No. 6. - P. 915 - 924.
14. *Коломиец В.М.* Приближение локальной плотности в атомной и ядерной физике. - К.: Наук. думка, 1990. - 164 с.
15. *Коломиец В.М.* Квантовая ядерная гидродинамика в приближении среднего поля // Ядерная физика. - 1983. - Т. 37, № 3. - С. 547 - 557.
16. *Hillery M., O'Connell R.F., Scully M.O., Wigner E.P.* Distribution functions in physics: Fundamentals // Phys. Rep. - 1984. - Т. 106, № 3. - P. 121 - 167.
17. *Ballentine L.E.* Quantum mechanics: A modern development. - World Scientific, 1998. - 676 p.
18. *Лифшиц Е.М., Питаевский Л.П.* Физическая кинетика. - М.: Наука, 1979. - 527 с.
19. *Baym G., Pethick C.J.* Landau Fermi Liquid Theory. - New York: J. Wiley & Sons, 1991. - 200 p.
20. *Abrikosov A.A., Khalatnikov I.M.* The theory of a Fermi liquid // Rep. Prog. Phys. - 1959. - Vol. 22. - P. 329 - 367.

21. *Fuls D.C., Kolomietz V.M., Lukyanov S.V., Shlomo S.* Damping effects on centroid energies of isoscalar compression modes // Europ. Phys. Lett. - 2010. - Vol. 90. - P. 20006(6).
22. *Kolomietz V.M., Lukyanov S.V.* A-dependence of enhancement factor in energy-weighted sums for isovector giant resonances // Phys. Rev. C. - 2009. - Vol. 79, No. 2. - P. 024321(5).
23. *Kolomietz V.M., Plujko V.A., Shlomo S.* Collisional damping in heated nuclei within Vlasov - Landau kinetic equation // Phys. Rev. C. - 1995. - Vol. 52, No. 5. - P. 2480 - 2487.
24. *Kolomietz V.M., Plujko V.A., Shlomo S.* Interplay between one-body and collisional damping of collective motion in nuclei // Phys. Rev. C. - 1996. - Vol. 54, No. 6. - P. 3014 - 3024.
25. *Di Toro M., Kolomietz V.M., Larionov A.B.* Isovector vibrations in nuclear matter at finite temperature // Phys. Rev. C. - Vol. 59, No. 6. - P. 3099 - 3108.
26. *Коломиец В.М., Константинов Б.Д., Струтинский В.М., Хворостьянов В.И.* К теории оболочечной структуры ядер // ЭЧАЯ. - 1972. - Т. 3, № 2. - С. 392 - 435.

В. М. Коломієць

НЕ-МАРКІВСЬКА ЯДЕРНА ДИНАМІКА

Пропонуються рівняння руху для параметрів форми ядра, що встановлюють прямий зв'язок ефектів пам'яті з динамічним збуренням поверхні Фермі. Рівняня руху для краплини ядерної фермі-рідини отримуються з використанням зіштовхувального кінетичного рівняння. У загальному випадку отримані рівняння є не-марківськими. Ефекти пам'яті пов'язані тут із збуренням поверхні Фермі і залежать від часу релаксації. Головна мета роботи полягає в застосуванні не-марківської динаміки до опису ядерних мультипольних гігантських резонансів і колективного руху з великою амплітудою. Ми беремо до уваги також дію випадкових сил і концентруємось на формуванні консервативних і дисипативних сил при колективному русі, що дає змогу більш чітко виявити вплив ефектів пам'яті на ядерну динаміку. У цьому відношенні запропонований підхід являє собою узагальнення традиційної моделі рідкої краплі на випадок краплини ядерної фермі-рідини. При практичному застосуванні ми приділяємо особливу увагу опису спуску ядра з бар'єра поділу до точки розриву.

Ключові слова: фермі-рідина, мультипольні гігантські резонанси, ядерний поділ, ефекти пам'яті.

В. М. Коломиец

НЕ-МАРКОВСКАЯ ЯДЕРНАЯ ДИНАМИКА

Предлагаются уравнения движения для параметров формы ядра, которые устанавливают прямую связь эффектов памяти с динамическим искажением поверхности Ферми. Уравнения движения капли ядерной ферми-жидкости получаются из столкновительного кинетического уравнения. В общем случае полученные уравнения есть не-марковскими. Эффекты памяти связаны здесь с искажением поверхности Ферми и зависят от времени релаксации. Основная цель работы состоит в применении не-марковской динамики к описанию ядерных мультипольных гигантских резонансов и коллективного движения с большой амплитудой. Мы учитываем также действие случайных сил и сосредоточиваемся на формировании консервативных и диссипативных сил в процессе коллективного движения, что позволяет более четко выявить влияние эффектов памяти на ядерную динамику. В этом отношении предложенный подход является обобщением традиционной модели жидкой капли на случай капли ядерной ферми-жидкости. При практическом применении мы уделяем особое внимание описанию спуска ядра с барьера деления до точки разрыва.

Ключевые слова: ферми-жидкость, мультипольные гигантские резонансы, ядерное деление, эффекты памяти.

Received 09.09.11,
revised - 09.11.11.